

Oceanic fronts along 45°E across Antarctic Circumpolar Current during austral summer 2004

N. Anilkumar^{1*}, M. K. Dash¹, A. J. Luis¹, V. Ramesh Babu², Y. K. Somayajulu², M. Sudhakar¹ and P. C. Pandey¹

¹National Centre for Antarctic and Ocean Research, Headland Sada, Goa 403 804, India

²National Institute of Oceanography, Dona Paula, Goa 403 004, India

A pilot expedition was launched to monitor the oceanic fronts in the southwestern sector of the Indian Ocean during January–February 2004. Major fronts along 45°E between 40 and 56°S were delineated and their spatial variations during 6–17 February have been compared with earlier studies. The Agulhas Return Front (ARF) has been identified between 40°15' and 41°15'S with a change in temperature from 19 to 17°C and a change in salinity from 35.54 to 35.39‰ at the surface. The position of Subtropical Front (STF) was observed between 41°15' and 42°15'S, with a rapid decrease in surface temperature from 17 to 10.6°C and salinity from 35.35 to 34.05‰. The Subantarctic Front has been located between latitudes 42°30' and 47°S, with a change in surface temperature from 9.7 to 6.3°C and change in surface salinity from 34.0 to 33.85‰. One of the significant findings here compared to previous studies is the identification of ARF and STF with almost equal width of ~110 km. In addition, the Surface Polar Front and the Subsurface Polar Front were also identified between 48 and 52°S. Temperature minimum layer has been located between 49 and 56°S and extends from 150 to 200 m. Its existence has been attributed to the residue of the previous winter mixed layer capped by seasonal warming and freshening. The freshwater input thickness from 49 to 56°S was estimated to be 55 ± 15 cm, with a major thickness (69 cm) at 54°S. It is suggested that the freshening south of the polar front could be due to the advection of melt water originating from the Weddell Basin.

THE Southern Ocean (SO) plays a prominent role in controlling the global ocean–atmospheric climate system¹. South Equatorial Current (SEC) and Antarctic Circumpolar Current (ACC) are two major surface current systems in the Southern Indian Ocean. Many oceanic frontal systems of various water masses south of the SEC are embedded in the eastward-flowing ACC system. Therefore, variability in these current systems can affect the climate. However, knowledge of the frontal systems, current pattern and water masses within the SO need to be improved to enhance the predictive capability of the general circulation and climate. The present investigation is carried out with an aim to understand the upper-ocean thermohaline structure

of the SO as well as to augment the data gaps and enhance our knowledge regarding the positioning and structure of oceanic fronts.

One of the major problems that hamper a comprehensive understanding of the physical and dynamical processes of the SO is the scarcity of *in situ* data from the western Indian Ocean during all seasons. It is to be noted here that studies of surface oceanic fronts in different meridional sections (42.5, 43.4, 45.9 and 49.2°E) in the vicinity of the present study region were carried out during austral summers of 1993 to 1995 elsewhere². Areas west of the Crozet Plateau are the key regions where the fronts confluence and split³. Hence, synoptic surveys of these areas deserve highest priority in any programme of observational studies of the South Indian/Antarctic Ocean^{3–5}.

The present investigation focuses on identification and delineation of frontal characteristics based on the thermohaline structure sampled along the ship track traversing the subtropical to polar waters (40 to 56°S) during 6–17 February 2004. The freshwater input south of 49°S was also computed to provide additional information based on the salinity data collected from the polar waters.

The National Centre for Antarctic and Ocean Research (NCAOR), Goa has initiated a Pilot Expedition to SO on-board ORV *Sagar Kanya* during austral summer 2004. Under this programme, the following *in situ* observations were made along 45°E.

The sea surface temperature (SST) was recorded using outboard bucket thermometer (accuracy: ± 0.2°C). Temperature and salinity profiles were measured at 1° intervals using CTD (make: SBE 9/11; accuracy: temperature ± 0.001°C, conductivity ± 0.0001 S/m and depth ± 0.005% of full scale). Salinity values were calibrated with the help of an Autosal (make: Guild line, model: 8400A) using the *in situ* samples collected at selected depths with Rosette samplers attached to the CTD.

The CTD observations were taken at every 1 m depth up to 760 m at 1° lat. interval from 40 to 56°S (Figure 1). Using these data, thermal and salinity structures were drawn to identify and study the characteristics of the fronts. Because of the variable nature of surface waters, it is not easy to classify each front based on an exact change in characterizing parameters. We follow the identification criteria for fronts used by other investigators^{2–9}. The adopted property indicators for identification of fronts are given in Table 1.

The freshwater input in the surface layer relative to Winter Water (WW) along the 45°E section was estimated using the formula¹⁰:

$$h = \frac{D_c(S_w - S^{\text{bar}})}{S_w}, \quad S^{\text{bar}} = \frac{1}{D_c} \left[\int_{-D_c}^0 S dz \right],$$

where h is the thickness of the freshwater input per unit surface area, D_c is the WW depth, S_w is the WW salinity,

*For correspondence. (e-mail: anil@ncaor.org)

Table 1. Adopted property indicators for identification of fronts

Frontal structure	Adopted criteria	
	Temperature (°C)	Salinity (‰)
Agulhas Return Front	19 ~ 17 at surface 10°C isotherm from 300 to 800 m	35.54 ~ 35.39 at surface 35.57 ~ 34.90 at 200 m
Subtropical Front	17 ~ 10.6 at surface 12 ~ 10 at 100 m	35.35 ~ 34.05 at surface 35 ~ 34.6 at 100 m 34.92 ~ 34.42 at 200 m
Subantarctic Front	9.7 ~ 6.3 at surface 8 ~ 5 at 200 m	34.0 ~ 33.85 at surface 34.40 ~ 34.11 at 200m
Polar Front (surface)	5.5 ~ 2.7	33.80 ~ 33.90 at surface
Polar Front (subsurface)	Northern limit of 2°C isotherm below 200 m	No variation*

*See text.

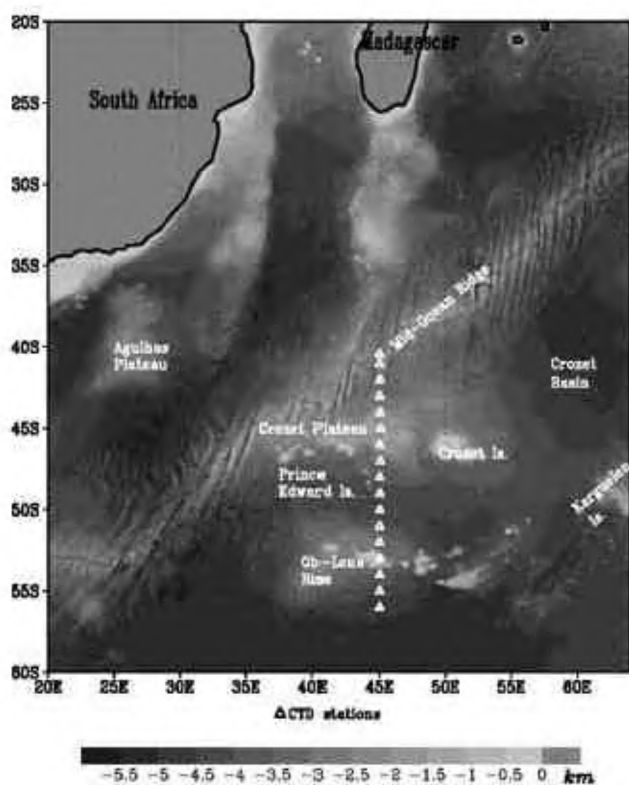


Figure 1. CTD station locations that were occupied (from south to north) during 6–17 February 2004.

and S^{bar} is the depth averaged salinity between the surface and WW depth.

Based on the literature criteria which are summarized in Table 1, we discuss below the various oceanic fronts and thermohaline characteristics in the SO waters.

Figure 2a and b depicts that in the region between 40°15' and 41°15'S, the surface temperature ranges from 19 to 17°C and the depth of the 10°C isotherm ranges from 300 to 750 m. The salinity ranges from 35.54 to 35.39‰

at surface and from 35.57 to 34.90‰ at 200 m in the region mentioned above (Table 1). Following the literature²⁻⁴, these typical characteristics indicate the presence of the Agulhas Return Front (ARF), which is the northernmost front in the meridional section along 45°E. Here, the ARF was identified as a distinct feature different from the Subtropical Front (STF), even though it was found to be close to STF. However, most of the earlier studies²⁻⁴ showed a clear resemblance with signatures of ARF identified here and our meridional section apparently has a distinct latitudinal position of ARF in the following respects. We observed the position of ARF between 40°15' and 41°15'S with a width of ~ 110 km, whereas its latitudinal position has been reported³ to be between 38 and 39°S. Similarly, its width has been documented² to be in the range of 44 to 73 km along other meridional sections (42.5, 45.9 and 49.2°E).

The ARF and STF are characterized by sharp and consistent surface expressions that make their identification relatively easy. In the present investigation, the location, for STF was identified between 41°15' and 42°15'S (Figure 2a and b). This identification is based on the following criteria^{2,4} (Table 1). Decrease in temperature at the surface was from 17 to 10.6°C (decrease in temperature at 100 m is from 12 to 10°C between 41°45' and 42°S) and the surface salinity ranged from 35.4 to 34‰ (salinity ranged from 35 to 34.6‰ at 100 m and from 34.92 to 34.42‰ at 200 m). The vertical profile of temperature (salinity) showed a surface value of 13.5°C (34.64‰) at 42°S (Figure 3a), which conforms to the criteria for identification of STF. In this study, the width of STF was observed to be ~ 110 km. The STF separates the subtropical surface waters from the subantarctic surface waters of the ACC¹¹. In earlier studies, many investigators described STF as a broad Subtropical Frontal Zone (STFZ)^{3,12,13} of more than 2° lat. Contrary to these earlier findings, the present analysis suggests that the STF is a narrow front of ~ 110 km.

From the thermal structure and salinity structure, the latitudinal position of the Subantarctic Front (SAF) was

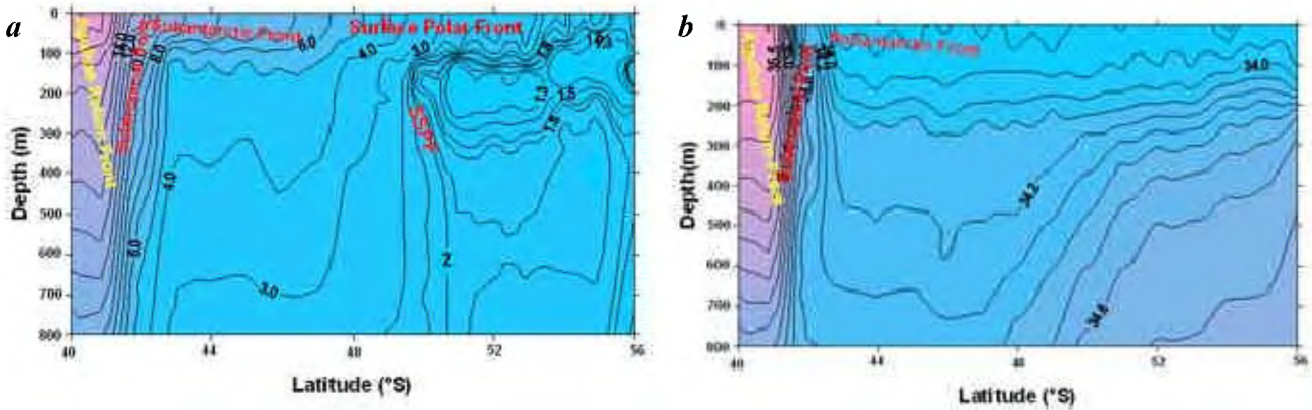


Figure 2. Thermal structure (a) and salinity structure (b) along 45°E.

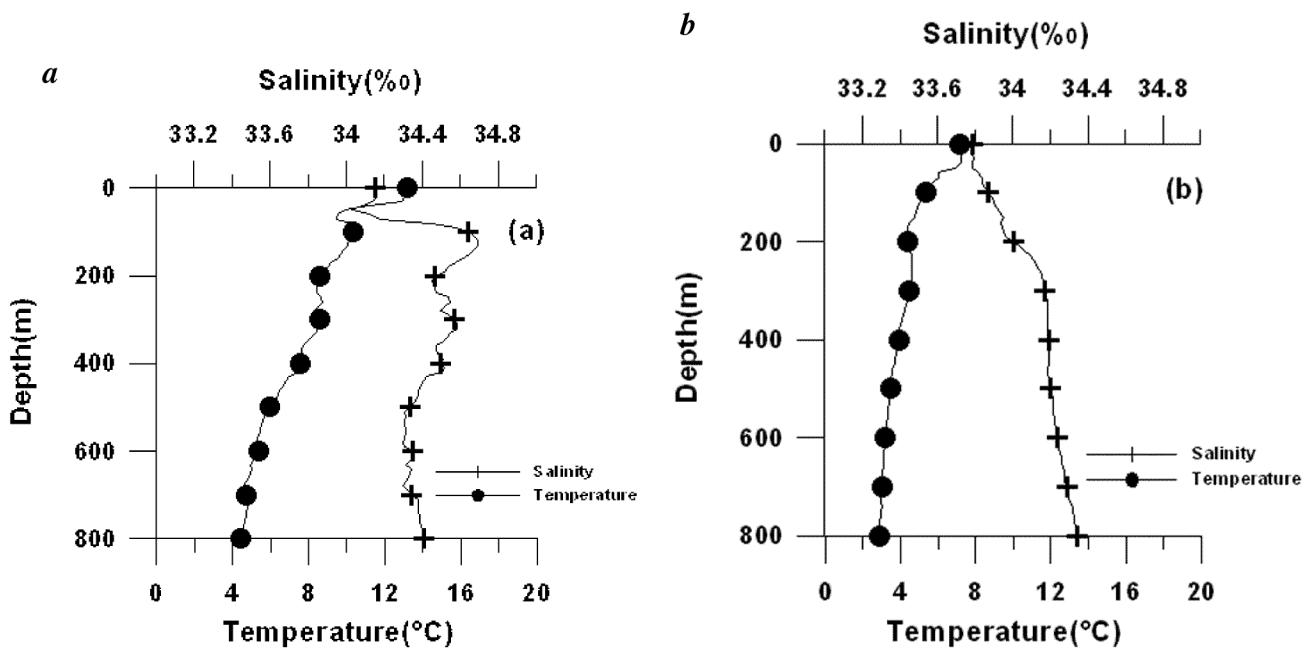


Figure 3. Vertical profile for salinity and temperature at (a) 42°S, 45°E and (b) 47°S, 45°E.

observed between 42°30' and 47°S (Figure 2 a and b). Between these latitudes, the surface temperature reduced from 9.7 to 6.3°C and the temperature at 200 m ranges from 8 to 5°C. Salinity varied from 34.0 to 33.85‰ at the surface (Figure 2 b and 3 b) and from 34.40 to 34.11‰ at 200 m (Table 1). The vertical temperature and salinity profiles at 47°S revealed that the temperature was 4°C at 200 m (Figure 3 b), while the surface salinity exhibited nearly a constant value of 33.85‰ (Figure 3 b). Hence all the above features (thermohaline structure and vertical profiles) strongly support the presence of the SAF. Our findings conform to the criteria adopted by other investigators^{3,4,6,7,9} and reveal a remarkable characteristic of the SAF. In this study, the SAF exhibited a width of ~500 km which is greater than the width of 165 and ~275 km observed by previous investi-

gators^{2,12} respectively. In brief, our data show a latitudinal variation in the position of SAF when compared with the previous studies^{2-4,13}.

From 48 to 52°S, we observed that the surface temperature reduced from 5.5 to 2.7°C and the northern limit of the 2°C isotherm was below 200 m (Figure 2 a). The above findings are analogous to the criteria employed to identify the Polar Front (PF) elsewhere²⁻⁴. Hence in this investigation, the PF was further split into two fronts: (i) Surface PF (SPF) and (ii) Subsurface PF (SSPF). The SPF is characterized by a fall in surface temperature from 5.5 to 2.7°C from 48 to 52°S, while the SSPF was identified by the northern limit of the 2°C isotherm below 200 m (Table 1). In the present study at the surface and subsurface, the variation in salinity was found to be insignificant in the

PF region (Table 1 and Figure 2 *b*). Hence the SPF and SSPF were identified using the temperature criterion. Surface salinity is not a reliable indicator of the presence of the PF as reported elsewhere². The average changes in the surface temperature of the PF (5.5–2.7°C) showed a marginal difference when compared with Holliday and Read² (5.8 ~ 2°C), Sparrow *et al.*⁴ (5 ~ 3.8°C), and Lutjeharms and Valentine¹² (4.1 ~ 2.5°C). A significant finding from our analysis of the present data was the identification of SPF between 48 and 52°S with a width of ~440 km, compared to the earlier studies^{2–4}. Earlier investigators² identified PF merged with SAF, with a latitudinal width of 29 km along 43.4°E. In another study³, PF was identified between 48 and 49°S along 45°E. In brief, it is found that the latitudinal positions of PF identified by us are marginally apart from the those of earlier studies.

In the present expedition the actual observation period for CTD data collection was only 12 days (6–17 February 2004) from 40 to 56°S, even though the total ship days taken for completion of the expedition was a longer duration of two months. Variation in surface temperature at the frontal regions observed in this study was compared with the Reynolds' SST¹⁴ (Figure 4). The evolution of fronts that we observed (Figures 2 *a* and 4) is discussed below. The ARF located with the Reynolds' SST showed a width of ~110 km (similar to the CTD observation). However, width of STF was >110 km (which was ~110 km based on the CTD data results). SAF (~500 km) and SPF (~440 km) were identified with almost similar width as that of the sea-truth observation.

We now discuss the thermohaline structure for the region south of the PF (52 to 56°S) with reference to Figure 2 *a*.

The vertical variation of temperature depicted interesting features in this region (Figure 2 *a*). A temperature minimum was identified between 100 and 200 m (reduction from surface values by 1.3°C) from 49 to 56°S. At 55°30'S, temperature inversion (~–0.815°C) was observed at 150 m. This subsurface minimum layer is attributed to the WW which was the residue of the previous winter mixed layer capped by seasonal warming and freshening¹⁰. Below this layer, the temperature increased gradually by ~2°C up to 350 m and further downwards, the temperature exhibited isothermal characteristics.

The WW depth (D_c) is defined as the WW core depth where the absolute minimum in subsurface temperature is observed¹⁰. The WW temperature decreased gradually to –0.815°C at 55°30'S. The freshwater layer thickness was computed from 49 to 56°S, since the temperature minimum layer was found in this latitudinal band. The freshwater layer thickness varied from 40 to 70 cm (Figure 5). The major input of freshwater was at 54°S and its layer thickness was 69 cm.

Based on the analysis of zonally-averaged net precipitation derived from the European Centre for Medium-Range Weather Forecasts, Bromwich *et al.*¹⁵ found a low value of precipitation (30 cm yr⁻¹) at 50°S. It was reported that south of 49°S along 30°E and 60°E and in the Kerguelen region, a decrease in surface salinity from spring to summer was found to have less influence on the regional precipitation^{10,16}. Hence based on the above findings it can be inferred that the net precipitation is not a cause for the freshwater input along 45°E. Another source for supply of freshwater in this region is from the melting of sea ice, which perhaps causes the spring/summer freshening in the subsurface layers due to the northward advection of melt water. Based on the salinity and oxygen isotope data col-

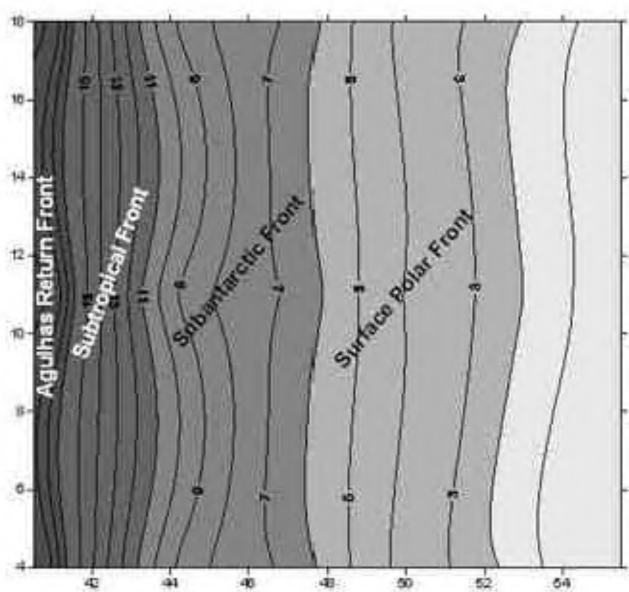


Figure 4. Weekly variation of Reynolds' sea surface temperature during 4–18 February 2004.

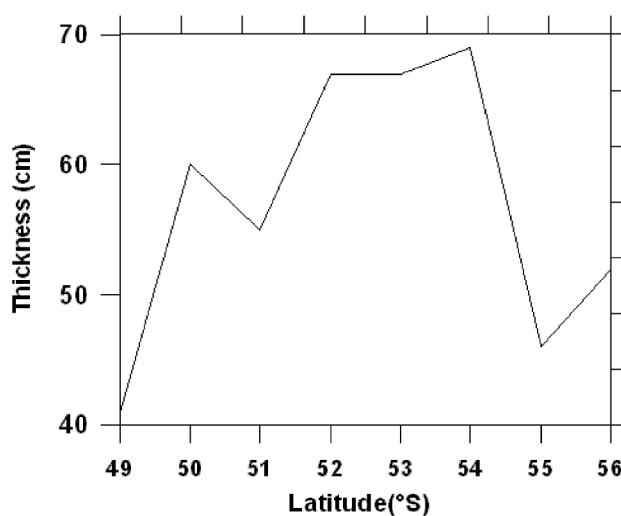


Figure 5. Estimates of freshwater thickness per unit surface area in the surface layer relative to winter water salinity from 49 to 56°S along 45°E.

lected along 30°E, it has been suggested that the surface layer freshening south of the PF is due to sea-ice melting, while that north of the PF is due to atmospheric precipitation¹⁷. Most extensive ice coverage was reported during winter in the Weddell Basin¹⁸. Hence we suggest that the advection of melt water from the south may be the source of freshwater south of the PF.

In this investigation we delineate the position and structure of the SO fronts: ARF, STF, SAF and PF based on the CTD data collected along 45°E during the Pilot Expedition to the SO. Except for a few studies, the western Indian sector of the SO has been poorly sampled and little is known about the frontal structure. Therefore, all the comparisons with our observations were made with those from the nearby areas. ARF was observed between 40°15' and 41°15'S with a width of ~110 km, contrary to narrower (44 and 73 km) ARF reported in an earlier study². However, STF was narrower (~110 km) compared to previous studies (> 220 km). On the other hand, the SAF was identified as a broader front (~500 km) compared to 165–275 km width reported by earlier studies^{2,12}. The difference in frontal positions between the present investigation and the earlier studies probably reveals the temporal variability of the fronts. One of the other important findings in this study is the identification of ARF and STF with almost equal width (~110 km). The ARF was more predominant in the surface as well as in subsurface layer. However, the isotherms depicting the STF showed a prominent variation in the surface layers. The PF was identified as SPF and SSPF. Another significant result is the identification of SPF between 48 and 52°S, with a width of ~440 km. The results of this analysis brought out the surface as well as subsurface manifestation of various oceanic fronts in a meridional section, which is not intensively examined so far in the present observational area. Temperature minimum layer was observed between 49 and 56°S as at 150 to 200 m, which is attributed to the WW. Computation of freshwater thickness reveals that the WW has a thickness of 55 ± 15 cm, which perhaps suggests a mesoscale activity between the PF and 56°S. This study suggests that the freshwater input in the southern part of study region may be due to the advection of melt water originating from the Weddell Basin.

6. Peterson, R. G. and Whitworth III, T., The Subantarctic and Polar Fronts in relation to deep water masses through the Southwestern Atlantic. *J. Geophys. Res.*, 1989, **94**, 10,817–10,838.
7. Orsi, A. H., Whitworth III, T. and Nowlin, Jr. W. D., On the circulation and stratification of the Weddell Gyre. *Deep-Sea Res. I*, 1993, **40**, 169–203.
8. Read, J. F. and Pollard, R. T., Structure and transport of Antarctic circumpolar current and Agulhas return current at 40°E. *J. Geophys. Res.*, 1993, **98**, 12281–12295.
9. Park, Y.-H., Gamberoni, L. and Charriaud, E., Frontal structure, water masses and circulation in the Crozet basin. *J. Geophys. Res.*, 1993, **98**, 12,361–12,385.
10. Park, Y.-H., Charriaud, E. and Fieux, M., Thermohaline structure of Antarctic surface water/winter water in the Indian sector of the Southern Ocean. *J. Mar. Syst.*, 1998, **17**, 5–23.
11. Deacon, G. E. R., The hydrology of the Southern Ocean. *Discovery Rep.*, 1937, **15**, 3–122.
12. Lutjeharms, J. R. E., Valentine, H. R., Southern Ocean thermal fronts south of Africa. *Deep-Sea Res.*, 1984, **31**, 1461–1475.
13. Lutjeharms, J. R. E., Location of frontal systems between Africa and Antarctica: Some preliminary results. *Deep-Sea Res.*, 1985, **32**, 1499–1509.
14. Reynolds, R. W. and Smith, T. M., Improved global sea surface temperature analysis using optimum interpolation. *J. Climate*, 1994, **7**, 929–948.
15. Bromwich, D. H., Robasky, F. M., Culather, R. I. and Van Woert, M. L., The atmospheric hydrologic cycle over the Southern Ocean and Antarctica from operational numerical analysis. *Mon. Weather Rev.*, 1995, **123**, 3518–3538.
16. Park, Y.-H., Charriaud, E., Ruiz Pino, D. and Jeandel, C., Seasonal and interannual variability of the mixed layer properties and steric height at station KERFIX, southwest of Kerguelen. *J. Mar. Syst.*, 1998, **17**, 233–247.
17. Archambeau, A. S., Pierrie, C., Poisson, A. and Schauer, B., Distribution of oxygen and carbon stable isotopes and CFC-12 in the water masses of the Southern Ocean at 30°E from South Africa to Antarctica: Results of Cival cruise. *J. Mar. Syst.*, 1998, **17**, 25–38.
18. Gloersen, P., Campbell, W. J., Cavalieri, D. J., Comiso, J. C., Parkinson, C. L. and Zwally, H. J., Arctic and Antarctic Sea Ice, 1978–87. Satellite passive-microwave observations and analysis. NASA SP-511, NASA, Washington DC, 1992, p. 290.

ACKNOWLEDGEMENTS. We are grateful to Dr Harsh K. Gupta, Secretary, Department of Ocean Development for his help in the implementation of this programme. Mr K. N. Babu and staff of NCAOR who participated in the SO cruise programme are acknowledged for their cooperation and help in the implementation of this project.

Received 10 September 2004; revised accepted 5 January 2005

1. Luis, A. J. and Pandey, P. C., Seasonal variability of QSCAT-derived wind stress over the Southern Ocean. *Geophys. Res. Lett.*, 2004, **31**.
2. Holliday, N. P. and Read, J. F., Surface oceanic fronts between Africa and Antarctica. *Deep-Sea Res. I*, 1998, **45**, 217–238.
3. Belkin, I. M. and Gordon, A. L., Southern ocean fronts from the Greenwich Meridian to Tasmania. *J. Geophys. Res.*, 1996, **101**, 3675–3696.
4. Sparrow, M. D., Heywood, K. J., Brown, J. and Stevens, D. P., Current structure of the South Indian Ocean. *J. Geophys. Res.*, 1996, **101**, 6377–6391.
5. Orsi, A. H., Whitworth III, T. and Nowlin, Jr. W. D., On the meridional extent and fronts of the Antarctic Circumpolar Current. *Deep-Sea Res. I*, 1995, **42**, 641–673.

***Agrobacterium*-mediated tomato transformation and regeneration of transgenic lines expressing *Tomato leaf curl virus* coat protein gene for resistance against TLCV infection**

S. K. Raj*, Rachana Singh, S. K. Pandey and B. P. Singh

Molecular Virology, National Botanical Research Institute, Lucknow 226 001, India

Coat protein (CP) gene of *Tomato leaf curl virus* (TLCV) was cloned into an expression vector and mobilized to *Agrobacterium tumefaciens* through triparental mating. Cotyledon leaf explants of Pusa Ruby tomato were transformed by co-cultivation with *Agrobacterium* containing TLCV-CP construct. Kanamycin-resistant transformants were regenerated and established in glasshouse. T0-generation putative transgenic plants obtained were screened by PCR, Southern and Northern hybridization tests and Western blot assay, which confirmed the incorporation and expression of the CP gene. CP expressing transgenic plants were self-pollinated. T1-generation transgenic plants were challenged by TLCV through whiteflies which showed variable degrees of disease resistance/tolerance compared to the untransformed control.

TOMATO (*Lycopersicon esculentum* L.) is an economically important crop in many countries, including India. *Tomato leaf curl virus* (TLCV) and *Tomato yellow leaf curl virus* (TYLCV) are the two major geminiviruses which cause serious losses to tomato production. Hence they are considered as major constraints and limiting factors for tomato cultivation. Therefore, tomato is an important target for introducing resistance against TLCV and TYLCV viruses.

Introduction of resistance genes found in wild tomato species into tomato cultivars had initiated the breeding for resistance¹. The first TYLCV field-tolerant cultivars showed mild or delayed symptoms^{2,3}. The potential of genetic engineering to produce geminivirus-resistant plants has been confirmed. Transformation of tobacco (*Nicotiana benthamiana*) plants with *Tomato golden mosaic virus* (TGMV) AC2 gene (necessary for virus replication) had shown a good level of resistance to TGMV infection³. Coat protein (CP) protection which has been successful and applied against several RNA viruses^{4,5}, was not reported to work with the geminiviruses till Kunik⁶ demonstrated that tomato plants transformed with TYLCV capsid protein were resistant to the virus. However, the transformation of tomato utilizing the CP gene of TLCV has never been attempted for developing transgenic tomato plants having in-built resistance against TLCV.

Therefore, we attempted tomato transformation through *Agrobacterium tumefaciens* using the CP gene of TLCV. The regenerated transgenic plants expressing the CP gene of TLCV have been found to be tolerant/resistant against TLCV under glasshouse conditions.

The TLCV CP gene-specific primers were designed from the available sequence data of DNA-A of TLCV^{7,8}. The primer sequences were: CP-I = 5'-ATGGCGAAGCGAC CAG-3' (I is the forward sequence from initiation codon) and CP-T = 5'-TTAATTTGTGACCGAATCAT-3' (T is the reverse complementary sequence from termination codon). The complete TLCV-CP coding region (771 bp) was amplified by PCR with these primers using cloned DNA-A of TLCV⁸. The PCR product was eluted through low melting point agarose electrophoresis and cloned into pROK2 expression vector at a *Sma*I site between the *Cauliflower mosaic virus* (CaMV) 35S promoter and NOS terminator⁹. The obtained construct (pROK-ITCP17) was mobilized into *A. tumefaciens* (strain LBA 4404) by triparental mating using a helper plasmid pRK 2013. The *Agrobacterium* conjugants were selected on 100 mg/l kanamycin and 100 mg/l rifampicin plates. Selected conjugants were screened by restriction digestion and PCR using TLCV-CP-specific primers. A positive conjugant containing the pROK-ITCP17 construct (Figure 1) was used for tomato transformation.

Healthy seeds of Pusa Ruby tomato were surface-sterilized and germinated on half MS medium¹⁰. Cotyledon explants of 14-day-old seedlings were used and transformation was done as described earlier^{11,12}. The sub-cuttings of explants made in MSO liquid medium were blot-dried and placed on full MS medium for two days preculturing. Simultaneously, *Agrobacterium* conjugant containing the construct (pROK-ITCP17) was grown for 48 h at 28°C, with shaking at 200 rpm in Luria broth (LB, Hi Media Laboratory, India) containing kanamycin (100 mg/l) and rifampicin (100 mg/l). The pre-cultured cotyledon discs were floated for 30 min in 1:15 dilution of *Agrobacterium* culture supplemented with 200 µM acetosyringone with gentle shaking in dark as described^{13,14}. The blot-dried explants were replaced on the same plate and incubated in dark for two days at 25°C. After co-cultivation, the cotyledonary leaf discs were transferred (placed upside-down) on selection medium (MS containing Gamborg's B5 vitamins, 50 mg/l ascorbic acid, 2.0 mg/l zeatin, 0.1 mg/l IAA, supplemented with 100 mg/l kanamycin and 500 mg/l cefotaxim). The plates were sealed with micropore tape and kept under regeneration at 25°C, with a 16 h/8 h (light/dark) photoperiod in the culture room. Sub-culturing was done at 3–4 weeks intervals and explants showing shoot regeneration were subsequently transferred to the same medium with a different hormone combination (0.1 mg/l zeatin and 0.1 mg/l IAA) for shoot development. The shoots obtained were transferred to rooting medium (MS containing Gamborg's B5 vitamins, 0.05 mg/l IBA and 50 mg/l kanamycin) for root development. Rooted plants were hardened in Hoagland's solution (containing 493 mg/l MgSO₄, 1180 mg/l Ca₂NO₃, 505 mg/l

*For correspondence. (e-mail: skraj2@rediffmail.com)